Laser-Induced Ablation through Nanometer-Sized Tip Apertures: Mechanistic Aspects†

Bertrand Dutoit,‡ Dieter Zeisel, Volker Deckert, and Renato Zenobi*

ETH Zürich, Laboratorium für Organische Chemie, Universitätsstrasse 16, CH-8092 Zürich, Switzerland

Received: April 30, 1997; In Final Form: July 1, 1997⊗

Mechanisms for laser ablation of rhodamine dye thin films through nanometer-sized tip apertures commonly used for scanning near-field optical microscopy (SNOM) are discussed. Experiments and observations are presented that refute a mechanism based on transient tip elongation. Ballistic heat transfer is found to be insufficient for ablation of ionic solids such as rhodamine dyes. The most likely mechanism for creation of the nanoindentations on rhodamine films is photothermal ablation. It is further demonstrated that rhodamine is sublimating upon irradiation, is transported over considerable distances, and is redeposited. This may permit laser ablation through SNOM tips for nanosampling and nanoanalytical methods.

Introduction

Near-field optical techniques are becoming increasingly useful to address scientific problems in molecular biology,[1−3] semiconductor device physics,[4,5] and chemical analysis.[6,7] One approach to perform molecular analyses of surfaces with nanometer spatial resolution is to liberate molecules from the surface under investigation using a SNOM probe. The liberated molecules can then be analyzed with a separate trace analytical method. We have demonstrated previously that small (<100 nm fwhm) holes can be produced on surfaces of molecular crystals by using pulsed laser radiation guided to the surface through a SNOM tip.[8] In contrast, polymers exhibited structures reminiscent of melt craters under the same conditions.[7] In this context, the goals of the studies presented below were 2-fold: first, to determine the mechanism responsible for ablation of the sample surfaces; and second, to prove that true ablation takes place by collecting gas-phase molecules in the vicinity of the SNOM tip. The physical requirements for ablation, such as pulse energy, laser wavelength, laser pulse energy coupled into the SNOM tip, etc., are also of interest in this context and are discussed.

Different mechanisms are possible for creation of holes or craters by pulsed laser radiation transmitted through nanometer-sized tip apertures. The simplest explanation is an axial expansion due to transient heating of the fiber tip. It can even be imagined that a small protrusion on the end of the tip can create indentations smaller than the overall tip diameter. A second possibility is ablation by energy transfer to the sample surface. Since the mean free path of nitrogen at atmospheric pressures is 68 nm, ca. 10 times larger than the typical distance between tip and sample, normal heat conduction is quite inefficient. We therefore assume the energy transfer to take place either by direct optical absorption in the film or by a ballistic mechanism,[9,10] mediated by ejection of adsorbed molecules (e.g., water) or atoms (e.g., aluminum from the coating) from the tip toward the sample.

Experimental Section

Rhodamine dyes (rhodamine 6G, MW = 479.02, $\epsilon_{max} = 10.5 \times 10^4$ L mol^{-1} cm^{-1}; and rhodamine B, MW = 479.02, $\epsilon_{max} = 10.7 \times 10^4$ L mol^{-1} cm^{-1}) were used in the present study because they have well defined and strong optical absorption bands and are easily detected by fluorescence. Films for SNOM ablation experiments were prepared by slow evaporation at 8 °C from an ethanol solution. The resulting films were a few tens of micrometers thick and homogeneous and exhibited an average roughness of a few nanometers as measured by shear force imaging. The behavior of rhodamine 6G and B was identical in all the experiments described below.

The fiber used was a quartz multimode step index fiber (HCG-M0100T-10, Ensign Bickford Co., Laser Components, Olching, Germany) with a core diameter of 100 μm. This fiber allowed the transmission of UV power with very little attenuation (0.27 dB/m at 308 nm), and the coupling of laser light into its large core diameter was reliable and relatively efficient (12%). Nevertheless, all input energies given below are quoted without taking the coupling efficiency into account.

Etching of the probes is done by the protection layer method.[11] In this self-terminating technique, a fiber with its protective coating removed is dipped for 90 min into a two-component liquid consisting of an etching fluid (40% HF) and a protecting overlayer (e.g., an oil). The tip forms as the meniscus height of the etching fluid decreases along the shaft on the fiber. The use of different overlayers allows precise control over the final cone angles.[12] In a second step the fiber is metallized with aluminum for suppressing light leakage and for obtaining a defined aperture for near-field experiments with subwavelength resolution.

Coupling in 500 μW of input power on the cleaved end of the fiber led to ≤2.5 μW output power measured in the far field (∼3 mm from the tip), yielding a transmission coefficient of ≤0.5%. The highest transmission for ∼100 nm apertures was obtained with the largest cone angles (∼25°) but varied considerably with the tip geometry. For detailed topographic measurements of surfaces, fiber tips were produced with dibutyl ether as the protecting overlayer, leading to small cone angles (∼6°) and taper regions of ∼800 μm length.

A commercially available near-field scanning optical microscope (Aurora, Topometrix, Santa Clara) was the basic unit of our experimental setup. For topographic measurements and for maintaining a constant tip-to-sample distance, the shear force approach was used.[13,14] The regulation ensured an average distance of ∼10 nm between probe and surface.

For ablation and precise surface modification pulsed laser light from a Nd:YAG pumped optical parametric oscillator (MOPO 730, Spectra Physics, Mountain View, CA) with a pulse width of 3−6 ns and a variable wavelength in the visible was

* To whom correspondence should be addressed. FAX + 41-1-632 12 92. E-mail: zenobi@org.chem.ethz.ch.

† Dedicated to Prof. Dieter Seebach on the occasion of his 60th birthday.

‡ Current address: Institut de Microsystèmes, DMT, Ecole Polytechnique Fédérale de Lausanne, CH-1015 Lausanne, Switzerland.

⊗ Abstract published in *Advance ACS Abstracts,* August 15, 1997.

S1089-5647(97)01454-5 CCC: $14.00

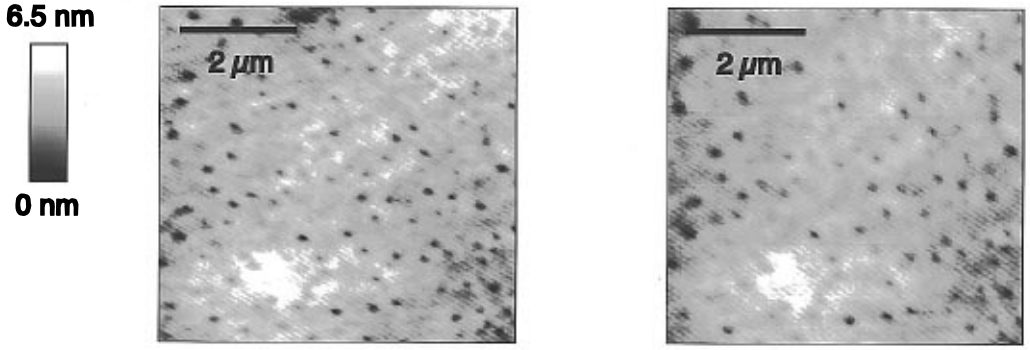

Figure 1. Topography of a 6 × 6 μm area of a rhodamine B film before (left panel) and after (right panel) attempts to ablate molecules from the film, using 60 μJ pulses coupled into a completely metallized SNOM tip. The total topographic contrast in the *z* direction is 6.5 nm.

coupled into the cleaved end of the fiber. The MOPO laser was operating at 20 Hz repetition rate, too fast for the production of distinct ablation craters if the SNOM was operated at its normal scanning speed ($\leq$2 lines/s). Hence, an electronically controlled shutter was used as a laser pulse selector, yielding either single shots or a reduced laser repetition rate between 0.5 and 10 Hz.

Rhodamine deposited from the gas phase onto uncoated SNOM tips was detected with fluorescence, excited by coupling 500 μW of the 514 nm line from an argon ion laser (532R-AP-A01, Omnichrome, Chino, CA) into the blunt end of the fiber. The fluorescence was collected by imaging the SNOM tip onto the entrance slit of a high-*f*-number spectrograph (Holospec f/1.8i, Kaiser Optical Systems, Ann Arbor, MI). Most of the excitation light was blocked by a holographic notch filter (Kaiser) inside the spectrograph. The dispersed light was detected by a liquid nitrogen cooled CCD camera (Photometrics, Tucson, AZ). The horizontal axis of the CCD chip represented the wavelength distribution of the fluorescence. The vertical axis represented the intensity distribution along the slit of the spectrograph, and was used to estimate the amount of material deposited along the axis of the tip.

Results and Discussion

(a) Ablation Mechanism. In the transient experiments one has to take thermal expansion[15,16] into account as a possible mechanism for the creation of surface indentations, but it is likely not to be the dominating mechanism. This result is based on four lines of evidence. First, electron micrographs of tips used for ablation showed overall tip diameters 2−3 times larger than the structures created on the surface. Second, the tips were not destroyed by their thermal expansion in the *z* direction during or shortly after the laser pulses, indicating a noncontact mechanism. Third, no disturbance of the shear force feedback loop was observed when laser pulses were transmitted through the SNOM tips. The feedback of the Aurora instrument works with a speed of 10 kHz, i.e., data points are available every 100 μs. If a significant tip elongation would take place, it should happen on the time scale of the laser pulse, i.e., within about 10 ns. The subsequent relaxation, however, is governed by material properties of the SNOM tip, in particular its thermal conductivity, which is low ($\beta_{glass} = 5 \cdot 10^{-7}$ K^{-1}). La Rosa et al.[17] found the thermal relaxation times of SNOM tips to lie in the range 8−16 ms, independent of the tip shape, the aluminum coating thickness, and the laser power coupled into the tip. Such a long relaxation time could be sampled very well, at least 100 times, by the shear force feedback loop. However, no regulation of the distance was observed during scans with laser shots, consistent with a negligible contribution from transient elongation of the SNOM tip.

The fourth argument is based on an experiment where laser pulses of relatively high energy were coupled into a completely metallized tip. We have previously observed ablation of an anthracene crystal surface to occur with such tips.[8] Typically, between 0.6 and 1.4 μJ coupled into the fiber were sufficient to cause ablation of anthracene by a ballistic heat-transfer mechanism. In Figure 1, the topography of the same 6 × 6 μm area of a rhodamine B film before (left panel) and after (right panel) attempts to ablate molecules from its surface is shown, using 60 μJ pulses coupled into the completely metallized SNOM tip. No ablation at all was found. These observations together strongly support a mechanism other than transient thermal expansion by the tip to be responsible for the small indentations.

The data presented in Figure 1 also argue against a ballistic ablation mechanism for the case of rhodamine dyes. "Ballistic" means that transient heating of the tip leads to ejection of atoms and molecules from the tip surface, which causes sputtering of the film underneath. This process is possible with completely metallized tips. For example, in nanoablation of anthracene and creation of nanometer-sized craters on polymer films, a ballistic mechanism was found to be the most likely explanation.[7] In the case of anthracene, a van der Waals solid, the enthalpy of sublimation is 104 kJ/mol.[18] A major difference between the samples used in the previous work and in the present study is that rhodamine is a chloride salt, expected to exhibit a higher enthalpy of sublimation and to require more drastic conditions for ablation by sputtering of atoms or molecules from the heated SNOM tip. Unfortunately, the heat of sublimation for rhodamine is not available in the literature. For other chloride salts, widely varying values are found. For example, CsCl has an enthalpy of sublimation of 164 kJ/mol,[19] 60% higher than that of anthracene. On the other extreme are values for overcoming the lattice energy (Madelung energy) for various chloride salts, which range as high as 1000 kJ/mol. In any case, greater energies are needed for sublimation of ionic solids compared to van der Waals solids, consistent with our observations.

Nanoablation by ballistic heat transfer was never observed on rhodamine films. At higher laser pulse energies, explosive disintegration of the SNOM tips occurred, as shown in Figure 2a. Above ca. 100 μJ input energy a flaking off of the tip's metal coating was observed, probably due to strongly different thermal expansion coefficients of glass ($\beta_{glass} = 5 \cdot 10^{-7}$ K^{-1}) and aluminum ($\beta_{alu} = 2.3 \cdot 10^{-5}$ K^{-1}). The damage threshold varied considerably, depending on the quality of the SNOM tips and their metal coating. If a sample was in close proximity to such an exploding tip, "giant" holes of several micrometers diameter induced by sputtering of aluminum could be observed in the rhodamine films, as shown in Figure 2b. A different tip than the one shown in Figure 2a was used to produce this crater.

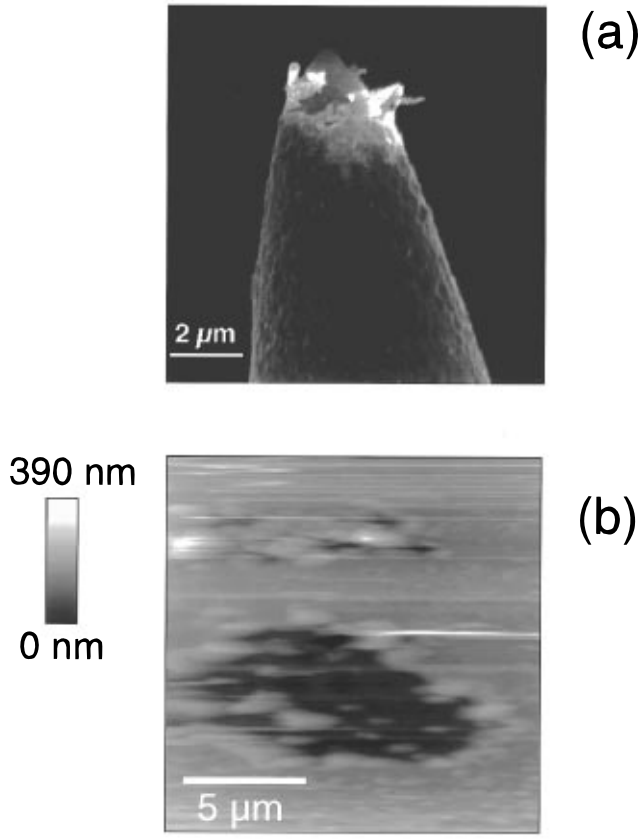

Figure 2. (a) Electron micrograph of a SNOM tip after coupling in ca. 100 μJ of laser energy in a 6 ns pulse at $\lambda = 450$ nm. (b) Giant hole created in a rhodamine B film by aluminum sputtering off from the coating. A different laser wavelength ($\lambda = 302$ nm) was used in (b) . The total topographic contrast in the *z* direction is 390 nm.

Often, deposition of small aluminum particles on the rhodamine film was observed after disintegration of a SNOM tip.

Experiments were also carried out to study the influence of the laser wavelength incident on molecular thin films. SNOM tips with apertures of about 100 nm diameter were used. No significant drop in optical output of the SNOM tip was measured for similar input energies at 400 and 650 nm input wavelength, although some decrease is expected due to the increasing difference between wavelength and tip aperture size. Figure 3 shows the absorption spectrum of rhodamine B in methanol solution (Figure 3a) as well as the shear force topography of a rhodamine B film recorded after attempts to ablate material from the film (Figures 3b,c). Two different ablation experiments were done, by coupling 2.1 μJ into the end of the SNOM tip far from the rhodamine B absorption band (at $\lambda = 650$ nm, Figure 3b), and after coupling 1.4 μJ into the fiber tip near the absorption maximum ($\lambda = 532$ nm, Figure 3c).

The topographic images were recorded in a subsequent scan after the laser pulses had been fired at the sample. No ablation was observed for an off-resonance wavelength (Figure 3b). In contrast, well defined $\leq$100 nm diameter, 5 nm deep holes were created by a wavelength that is strongly absorbed by the sample. This clearly points to an optical ablation mechanism, either photochemical or photothermal. Also, energy transfer by absorption of photons appears to be more efficient than by a ballistic process. The photon energy used here is not sufficient for inducing chemical bond dissociation in the rhodamine film, in contrast to ablation processes with ultraviolet laser radiation, where a photochemical ablation mechanism is often used to rationalize the observed phenomena.[20] We therefore suggest that a photothermal mechanism is responsible for the ablation

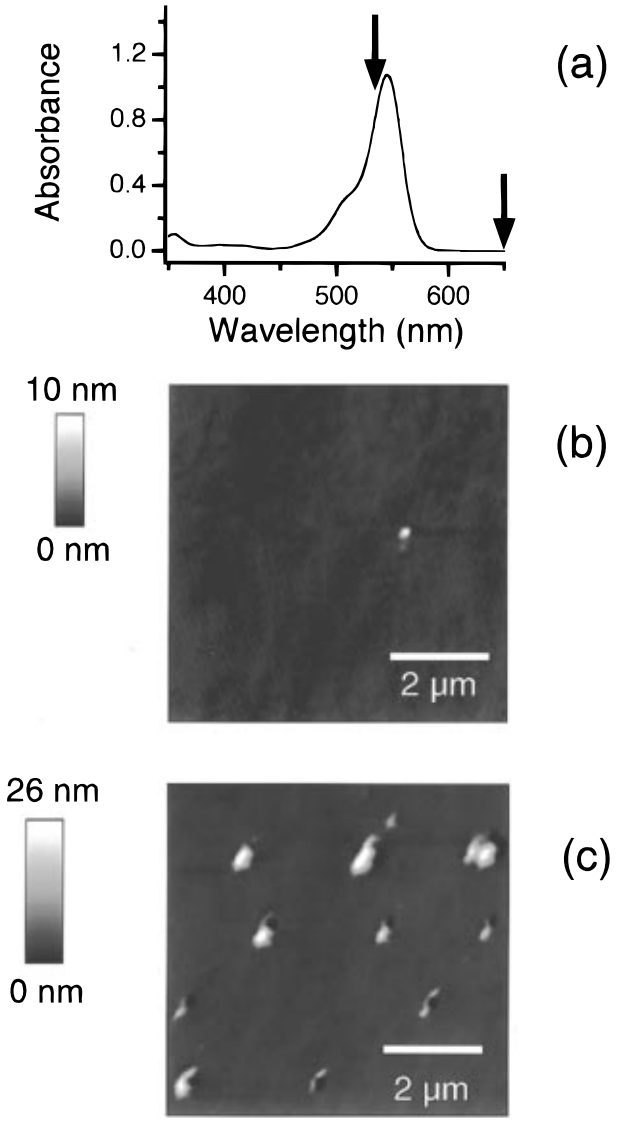

Figure 3. (a) Absorption spectrum of rhodamine B at a concentration of 10^{-5} M in methanol solution. Arrows indicate the wavelengths used for the ablation experiments before recording the images shown below. (b, c) Topography of a rhodamine B film after coupling 2.1 μJ into the SNOM tip at $\lambda = 650$ nm (b), and after coupling 1.4 μJ into the SNOM tip at $\lambda = 532$ nm (c), a wavelength near the maximum absorption of rhodamine B. The total topographic contrast in the *z* direction is 10 nm (b) and 26 nm (c), respectively.

of the organic films: we believe that the absorbed photon energy is converted to vibrational excitation, causing a rapid temperature increase that leads to thermal desorption of the molecules.

From the absorbance of rhodamine B, an optical penetration depth of $\approx$20 nm can be estimated at 532 nm, about 4 times the measured hole depth. The latter may be underestimated in the shear force topographic data,[21] due to some convolution with the tip shape. The characteristic thermal diffusion length in the rhodamine film was estimated to be small, on the order of 100 nm for a laser pulse width of 5 ns. Because at this distance the temperature jump is reduced to 1/*e* of its maximum value and because ablation yields usually show a very strong dependence on temperature or even a threshold behavior, spreading of thermal energy is not expected to increase the ablated area substantially. This is consistent with the observed small size of the indentations. Calculating a near-field ablation threshold for rhodamine was impossible, as too many parameters were not determined well enough. In far-field laser ablation studies, 160 mJ/cm^2 were needed for ablation of rhodamine dye

films using the second harmonic of a Nd:YAG laser,[22] consistent with a fairly high energy density requirement. The amount of redeposited material visible around the craters in Figure 3c varies considerably. Analysis of line sections shows that this variation is correlated with the depth of the crater where the material came from. This variation can therefore be explained by shot-to-shot variations of the laser pulse energy, probably amplified by a nonlinear irradiance dependence of the ablation yield.

(b) Detection of Vapor Phase Rhodamine. The possibility of vaporizing molecules from a surface is of great practical usefulness for analytical nanosampling[23] and may therefore become important for the application of high transmission SNOM tips. The question of whether or not gas-phase material is released from the sample surface is also relevant for optical writing with SNOM technology, because redeposited solid debris may seriously degrade the surface quality. The data presented so far do not allow us to decide whether material from the sample surface is actually liberated or not. We therefore tried to collect gas-phase material in the vicinity of the ablation crater by precipitating it on a collection surface and detect it either by fluorescence or by secondary ion mass spectrometry (SIMS). The collection surface was either a cleaved fiber tip mounted on the sample surface at a small distance from the SNOM tip or the SNOM tip itself. Extensive blank studies were carried out to exclude detection of material that resulted from accidental touching of the sample or from contamination.

It was difficult to mount a cleaved fiber tip within less than 100 μm of the point of ablation. Attempts to detect rhodamine dyes on such collections surfaces either by SIMS, which has a detection limit of 10^{-4} monolayer, or by fluorescence microscopy were not successful. Fluorescence detection was additionally complicated by some residual emission of the fibers themselves.

We suspected that the SNOM tip itself blocks the escape of most of the vaporized material. Although it can be imagined that a high vapor pressure created between the tip and the sample will drive material out to the sides, perhaps in a preferred direction due to tip asymmetry, it must be kept in mind that the tip end has an overall diameter of 100−200 nm, while being only 5−10 nm from the surface during shear force feedback. We therefore carried out experiments to detect vaporized rhodamine 6G directly on a SNOM tip. The tips used here were uncoated to prevent quenching of the rhodamine 6G fluorescence by the aluminum coating. The ablation laser pulse energy coupled into the back of the fiber was 0.5 μJ at a wavelength of 532 nm. These fiber tips were quite blunt, which resulted in similar power density as in the experiments described above, due to an elevated optical transmission.

The results are shown in Figure 4. Many blanks were recorded (Figure 4a), by scanning both with relatively large distances between tip and sample (10−15 nm) and in near-contact mode ($\leq$7 nm). Even intentional touching of the dye film by the tip did not transfer any detectable material. Figure 4b shows the fluorescence detected on a SNOM tip after firing several laser pulses at a wavelength of 532 nm through the fiber, which was in feedback, i.e., a few nanometers from the dye film. A fluorescence signal from rhodamine 6G was clearly detected on this fiber tip after the ablation experiment. We interpret this finding as being due to transport of rhodamine 6G from the film to the tip via the vapor phase. With uncoated fiber tips it was impossible to obtain high spatial resolution for the ablation craters. A rather large (10 μm diameter) area was ablated, facilitating detection of the rhodamine fluorescence. By analyzing the CCD pixels in the vertical direction, it was also possible to estimate the spatial distribution of the rhodamine

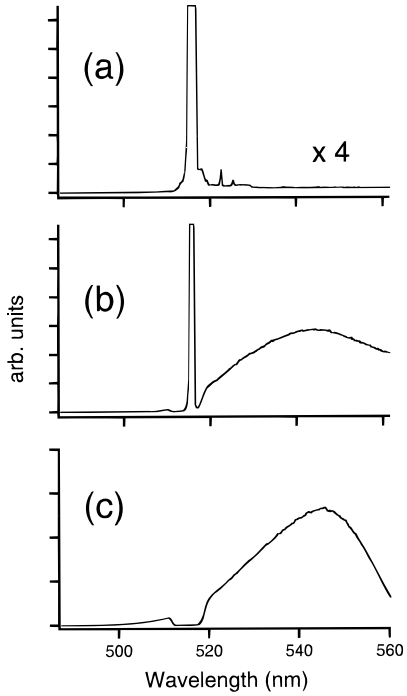

Figure 4. Fluorescence spectra (excitation wavelength 514 nm) recorded from the very end of a SNOM tip used for ablation. (a) Blank experiment. (b) Several 0.5 μJ laser pulses (λ = 532 nm) were coupled into the fiber to create a large (10 μm diameter) ablation crater on the surface of a rhodamine 6G film. The exposure in (a) was different than in (b), leading to saturation of a larger number of pixels on the CCD chip, and a larger apparent width of the excitation line. (c) Fluorescence spectrum of a rhodamine 6G film, for reference.

6G on the tip. A concentration that decreased from the end of the tip toward the shaft was found, consistent with a sublimation−redeposition mechanism. We cannot exclude that some large chunks of rhodamine 6G are sputtered away from the surface simultaneously, although the distribution along the tip in the vertical direction was more consistent with redeposited gas-phase material.

A fluorescence spectrum of a rhodamine 6G film is given in Figure 4c for comparison. Note that none of the spectra in Figure 4 are corrected for spectral dependencies of the optics, the grating, and the CCD camera, giving rise to an overestimation of the fluorescence in the blue side of the band and a shift of the emission maximum to the left. The spectrum in Figure 4c was recorded by guiding the fluorescence from the film to the spectrograph with fiber optics. This difference in imaging geometry and the fact that the fluorescence from the intact dye film was much more intense than in the case of ablated dye explain the somewhat steeper decrease toward the red and the absence of the excitation laser line in (c). The spectral resolution for recording spectra (a)−(c) was equal. The difference in the apparent width of the excitation laser line in (a) and (b) is due to saturation of single CCD pixels, which was reached more easily in spectrum (a) due to a longer exposure time. The similarity between the spectrum of the fresh film (Figure 4c) and the spectrum of the ablated rhodamine 6G shows that intact material is transported from the film to the tip by photoablation.

If vaporization takes place, the method becomes attractive for liberating material to be transported over larger distances and analyzed subsequently by a trace analytical method. Transport over distances of many micrometers was indeed observed in several cases. The result of such an experiment is shown in Figure 5. Here an anthracene crystal surface was continuously irradiated with 6 ns, 532 nm, 50 μJ pulses from a laser operated at 20 Hz repetition rate during a 1 × 2 μm scan.

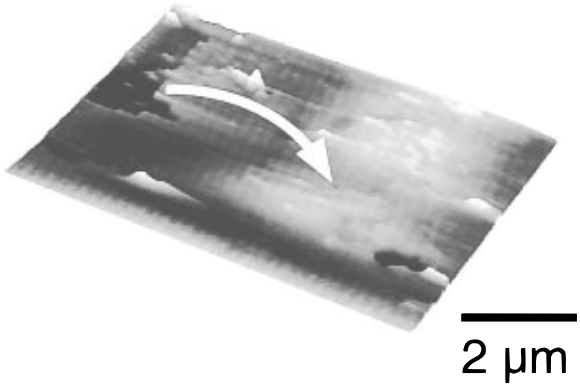

Figure 5. Transport of material over many micrometers: 5×8 μm area of an anthracene film surface, irradiated previously at 20 Hz repetition rate with 6 ns, 532 nm, 50 μJ laser pulses. Total topographic contrast is 100 nm.

A shear force image of a larger area was then recorded without irradiation. A $\approx$1 μm wide trench with well-defined edges could be detected in the upper part of the image, while a 2 μm wide, 60 nm high hill was found about 5 μm away, parallel to the trench. We interpret this again as vaporization−redeposition of material, but into a preferred direction, most likely determined by an asymmetric shape of the tip used. The same phenomena can also be observed, though to a lesser extent, in Figure 3b: all the protrusions found after the ablation experiment have approximately the same shape and lie in the same orientation around the circular craters. It is important to realize that the direction of the material transported was independent of the scan direction. From Figure 5 we also estimate that only few large chunks of material are ejected. Most of the anthracene is found in the form of a diffuse and structureless hill, which is expected if the molecules are redeposited form the gas phase. We conclude that material transport does not take place by mechanical dragging, but through vaporization and redeposition in a direction dictated by the details of the tip shape.

These findings allow to develop strategies for SNOM ablation followed by chemical analysis in a second step. The possibility to perform real ablation suggests that a SNOM tip could be successfully used as a sampling device for mass spectrometric analysis.[23] For example, micro- or nanopipets[24,25] may be used for suctioning the ablated material into a mass spectrometer ion source. Also, tips with specially engineered shapes could be designed for ejection of material into a predetermined direction. Finally, entire systems for chemical analysis[26] can now be integrated and miniaturized and may perhaps become a part of a multipurpose SNOM for chemical analysis if mounted very close to the tip.

Conclusions

We have investigated the mechanism for pulsed laser ablation of organic materials through SNOM tip apertures. It was shown that thermal expansion of the SNOM tip is not responsible for the craters generated. Two mechanisms were found to be important, direct photothermal ablation following absorption of the laser energy by the material, and ballistic heat transfer mediated by ejection of adsorbed molecules from the tip toward the sample. The ballistic mechanism is less efficient and was observed only on van der Waals solids. For strong optical absorbers the photothermal mechanism is very efficient and even leads to the ablation of ionic solids such as the rhodamine dyes studied. Finally, it has been shown that the ablated material is undergoing a solid−vapor phase transition and that it can be transported over many micrometers.

Acknowledgment. We wish to thank the Swiss National Research project "Nanotechnology" (NFP 36) managed by the Swiss National Science Foundation for financial support.

References and Notes

(1) Dunn, R. C.; Holtom, G. R.; Mets, L.; Xie, X. S. *J. Phys. Chem.* **1994**, *98*, 3094.
(2) Hwang, J.; Tamm, L. K.; Bohm, C.; Ramalingam, T. S.; Betzig, E.; Edidin, M. *Science* **1995**, *270*, 610.
(3) van Hulst, N. F.; Moers, M. H. P. *IEEE Eng. Med. Bio.* **1996**, *15*, 51 .
(4) Hess, H. F.; Betzig, E.; Harris, T. D.; Pfeiffer, L. N.; West, K. W. *Science* **1994**, *264*, 1740.
(5) Grober, R. D.; Harris, T. D.; Trautman, J. K.; Betzig, E.; Wegscheider, W.; Pfeiffer, L.; West, K. *Appl. Phys. Lett.* **1994**, *64*, 1421.
(6) Rosenzweig, Z.; Kopelman, R. *Anal. Chem.* **1995**, *67*, 2650.
(7) Zeisel, D.; Dutoit, B.; Deckert, V.; Roth, T.; Zenobi, R. *Anal. Chem.* **1997**, *69*, 749 .
(8) Zeisel, D.; Nettesheim, S.; Dutoit, B.; Zenobi, R. *Appl. Phys. Lett.* **1996**, *68*, 2491.
(9) Dransfeld, K.; Xu, J. *J. Microsc.* **1988**, *152*, 35.
(10) Xu, J.-B.; Läuger, K.; Möller, R.; Dransfeld, K.; Wilson, I. H. *J. Appl. Phys.* **1994**, *76*, 7209.
(11) Turner, D. R. US Patent no. 4,469,554, 1983.
(12) Hoffmann, P.; Dutoit, B.; Salathé, R.-P. *Ultramicroscopy* **1995**, *61*, 165.
(13) Betzig, E.; Finn, P. L.; Weiner, J. S. *Appl. Phys. Lett.* **1992**, *60*, 2484.
(14) Toledo-Crow, R.; Yang, P. C.; Chen, Y.; Vaez-Iravani, M. *Appl. Phys. Lett.* **1992**, *60*, 2957.
(15) Stähelin, M.; Bopp, M. A.; Tarrach, G.; Meixner, A. J.; Zschokke-Gränacher, I. *Appl. Phys. Lett.* **1996**, *68*, 2603.
(16) Lienau, C.; Richter, A.; Elsaesser, T. *Appl. Phys. Lett.* **1996**, *69*, 325 .
(17) La Rosa, A. H.; Yakobson, B. I.; Hallen, H. D. *Appl. Phys. Lett.* **1995**, *67*, 2597.
(18) Karcher, W.; Ellison, S. *Spectral atlas of polycyclic aromatic compounds*; Kluwer: Dordrecht, 1988; Vol. 2.
(19) Landolt-Börnstein. *Zahlenwerte und Funktionen aus Naturwissenschaft und Technnik*; Schäfer, K., Lax, E., Eds.; Springer: Berlin, 1961; Vol. 6, II/4.
(20) Singleton, D.; Paraskevopoulos, G.; Taylor, R. S. *Chem. Phys.* **1990**, *144*, 415 .
(21) Hecht, B.; Bielefeldt, H.; Inouye, Y.; Pohl, D. W.; Novotny, L. *J. Appl. Phys.* **1997**, *81*, 2492.
(22) Schilke, D. E.; Levis, R. J. *Rev. Sci. Instrum.* **1994**, *65*, 1903 .
(23) Kossakovski, D.; O'Connor, S. D.; Widmer, M.; Baldeshwieler, J. D.; Beauchamp, J. L. *Proceedings of Fourth International Conference on Near-Field Optics (NFO-4)*; Jerusalem, 1997; p 25.
(24) Lieberman, K.; Lewis, A.; Fish, G.; Shalom, S.; Jovin, T. M.; Schaper, A.; Cohen, S. R. *Appl. Phys. Lett.* **1994**, *65*, 648.
(25) Lieberman, K.; Lewis, A. *Appl. Phys. Lett.* **1993**, *62*, 1335.
(26) Manz, A.; Harrison, D. J. *Adv. Chromatogr.* **1993**, *33*, 1.